International Journal of Research Publication and Reviews

Advancements in Radio Refractivity Prediction for Tropical Environments using Artificial Neural Network

[1] P.C. Amalu, [2] O. Olabisi and [3]O. Adegboyega

[1]Department of Physics, Ajayi Crowther University, Oyo, Nigeria.
[2]Department of Science Laboratory Technology, Ladoke Akintola University of Technology, Nigeria and
[3]Department of Physics, Emmanuel Alayande university of Education, Oyo, Oyo state, Nigeria.
Email: oolabisi@lautech.edu.ng.

ABSTRACT

Radio refractivity prediction plays a crucial role in ensuring reliable communication in tropical regions where weather conditions significantly influence signal propagation. Traditional prediction methods face challenges due to the unique characteristics of tropical environments, such as high humidity levels, convective activities, and rapid weather changes. This study focuses on the development and application of ANNs for accurate and efficient radio refractivity prediction in tropical regions. Extensive data collection from meteorological stations and radio propagation measurements in tropical areas forms the basis of a comprehensive dataset used for training and validation. The ANNs are trained using this dataset, incorporating advanced algorithms, optimization techniques, and adaptive learning approaches to capture the complex relationships between meteorological conditions and radio refractivity. The results demonstrate that the ANN-based approach significantly enhances radio refractivity prediction in tropical environments. Compared to traditional methods, the ANN models offer improved accuracy, reduced errors, and enhanced forecasting capabilities. Real-time predictions provided by the ANNs enable adaptive communication systems to dynamically adjust to changing environmental conditions, ensuring reliable signal coverage and mitigating signal degradation. These advancements in radio refractivity prediction have significant implications for optimizing communication systems and designing robust networks in tropical regions. By leveraging the power of artificial neural networks, reliable communication can be ensured even in challenging tropical conditions. The findings of this study contribute to the advancement of prediction models for tropical environments and open up avenues for further research and innovation in the field.

Key words: Artificial Neural Network, meteorological parameters, Refractivity, Multipath effects, Troposphere

1.0 INTRODUCTION

Accurate prediction of radio refractivity is vital for effective telecommunications, particularly in tropical regions where weather conditions strongly impact signal propagation. This study introduces an advanced approach that leverages a modified artificial neural network (ANN) in conjunction with meteorological parameters to significantly improve the accuracy of radio refractivity predictions in these dynamic environments. The propagation of radio signals is influenced by atmospheric properties, leading to various behaviors such as scattering, absorption, reflection, and refraction [1]. Within the troposphere, the fundamental factors affecting radio links, frequency, and signal strength are atmospheric pressure, temperature, and relative humidity [5]. These factors contribute to variations in the refractive index of the troposphere, known as radio refractivity. Large-scale variations in atmospheric refractive index, such as horizontal layers with distinct refractivity, give rise to multipath effects [7]. This effect becomes noticeable when a signal takes multiple paths to reach its destination, with the resulting rays arriving at different times and interfering with each other during tropospheric propagation.

The substantial impact of these large-scale variations in tropospheric refractive index causes radio waves to gradually curve towards the Earth as they propagate through the atmosphere. Even slight variations in these parameters can significantly affect radio wave propagation, as the signals are refracted over the entire path, often leading to degradation of communication links [4][12]. This study focuses on measuring atmospheric pressure, temperature, and water vapor pressure, and employs an indirect method utilizing an empirical formula provided by the International Telecommunication Union to determine radio tropospheric refractivity. Additionally, the study demonstrates the application of a feed-forward back propagation artificial neural network (ANN) with hyperbolic tangent neurons in the hidden layer and linear neurons in the output layer. This ANN model is utilized to predict monthly radio refractivity in southwestern Nigeria.

1.1 THEORETICAL BACKGROUND

The radio refractive index is defined as the ratio of the speed of propagation of radio energy in a vacuum to the speed in a specified medium as shown in Equation **Error! Reference source not found.**

$$n = \frac{C_v}{C_m} \tag{1}$$

The refractive index of air, n, is measured by refractivity, N, and the two parameters are related as [2]

$$N = (n-1) \times 10^6 \tag{2}$$

The radio refractive index may be measured directly if the measuring instrument is sensitive to the speed of propagation. It is measured indirectly by measuring temperature, pressure, and humidity with subsequent conversion to the refractive index as shown below;

The radio refractivity is derived in terms of the primary weather parameters (Temperature, water vapour pressure and atmospheric pressure) using equation **Error! Reference source not found.**

$$N_{(T,P,e)} = N_{dry} + N_{wet} \tag{3}$$

where

$$N_{dry} = \frac{77.6P}{T} \tag{4}$$

$$N_{wet} = 3.732 \times 10^5 \frac{e}{T^2} \tag{5}$$

$$N_{(T,P,e)} = \frac{77.6P}{T} + 3.732 \times 10^5 \frac{e}{T^2} \tag{6}$$

Equation **Error! Reference source not found.** is used to determine radio refractivity up to the frequencies of 100 GHz with error less than 0.5%. [2]. The water vapour pressure, e, is quantified using Equation (7)

$$e = \frac{RH}{100} \, a \exp\left(\frac{bt}{t+c}\right) \tag{7}$$

where *RH* represents the relative humidity, *t* is the temperature (℃). Moreover, the coefficients are given as: $a = 6.1121$, $b = 17.502$, and $c = 240.97$. These coefficients are valid from −20 to 50 ℃ with an accuracy level $\pm 0.2\%$ [11], [8].

2.0 METHODOLOGY

The research methodology involves incorporating meteorological parameters, including temperature, humidity, atmospheric pressure, and precipitation, into a modified ANN framework. This modified ANN is specifically tailored to address the unique challenges posed by the tropical region, such as high humidity levels, convective activities, and rapid weather changes. By accounting for these factors, the model aims to accurately capture the intricate relationships between meteorological conditions and radio refractivity. An indirect approach was employed to measure radio refractivity, utilizing high-resolution radiosonde data obtained from the Nigerian Meteorological Agency (NiMeT) in Ibadan, southwestern Nigeria (7° 22' 39" N, 3° 54' 21" E). The meteorological dataset for the year 2021 consisted of air temperature, relative humidity, and atmospheric pressure recorded at the sounding balloon's height. To obtain representative data, the hourly measurements collected from January to December were averaged to yield twenty-four data points per day. Subsequently, the daily data points were further averaged to derive a single data point for each day, and finally, the monthly average was computed to capture the variations throughout the year. Using the obtained meteorological data, the surface radio refractivity was computed using Equation (6). While Nigeria's latitude falls within the tropical zone, the country exhibits diverse climatic conditions, with the northern regions experiencing arid conditions and the southern parts being more equatorial. The general weather pattern can be categorized into a wet season (August to February) and a dry season (March to July).

2.1 TREATMENT OF DATA AND DEVELOPMENT OF ARTIFICIAL NEURAL NETWORK

A minimum-maximum normalization process was performed on the inputs and preprocessed Radio refractivity dataset obtained along the three itineraries using equation **Error! Reference source not found.**. This was done to prevent impulsive changes due to large variation in the datasets

$$y = \frac{(y_{max} - y_{min}) \times (x_{in} - x_{min})}{(x_{max} - x_{min})} + y_{min} \tag{8}$$

Since $y_{min} = -1$ and $y_{max} = +1$, x_R is the original data, y is the result of normalization. Equation (8) becomes,

$$y = \frac{2(x_{in} - x_{min})}{(x_{max} - x_{min})} - 1 \tag{9}$$

the normalized parameters were subjected to the ANN algorithm for training the data. For any configuration to be trained, the algorithm used randomly splits the data into 70% for training, 15% for Test, and 15% for Validation. In this study, a single-layered Levenberg-Marquardt with feed forward back propagation learning algorithm ANN architecture which encompassed four input neurons and one output neuron was designed for model training and development, as shown in Figure 2. The ANN model design, training, validation, and testing were all done using a MATLAB 2020a produced by MathWorks Inc. Testing data-set comprised of data instances that are not included in the training data-set. The testing dataset was created to evaluate the generalization ability of the ANN models. The input data variables of the datasets include Temperature, relative humidity and atmospheric pressure.

The single target output of the ANN model is the corresponding path loss values. The values of the input parameters are fed into the neurons in the input layer, while the output parameter (Radio refractivity) which depends on input parameters is the predicted variable. In ANN, the output layer accepts its input from the last hidden layer. Several configurations were trained before arriving at the best configuration for the modeling. Tansig transfer function was used at the hidden layer while purelin transfer function was used at the output layer as shown in equation **Error! Reference source not found.**

$$y = \sum_{j=1}^{m} \left\{ Purelin\left[LW_{j,1}\left(\sum_{i=1}^{4} tansig(X_i IW_{i,j} + b_j) \right) \right] + b_o \right\} \tag{10}$$

where Wij (or IW) represents the weights for input layer to hidden layer and LW represents hidden layer to output layer weights, b_j is the bias value for jth hidden neurons and b_o represents the bias for output neuron. During the training process, the epochs and goals were used as the stopping criteria to regulate the number of iterations and error tolerance respectively. The training stops once either the epoch or goal is reached. For this study, an epoch of 1,000 and a goal of zero were set. After denormalization and recovery phases, actual and forecasted testing datasets were evaluated. The network output with optimal configuration $3 \times 5 \times 1$ is obtained as follows:

$$E_{1,i,j} = \sum_{i=1\ldots2}^{j=1\ldots9} W1_{i,j}x_j * W1_{1,1}X_1 + W1_{1,2}X_2 + W1_{1,3}X_3 \tag{11}$$

where , $W1_{1,1}$, $W1_{1,2}$, $W1_{1,3}$, refer to weights assigned to Temperature, relative humidity and atmospheric pressure respectively in the input (i) and for each neuron (j) in the hidden layer 1. The Tansig transfer function activates on $E_{1,i,j}$ to give $F_{1,i,j}$ defined as **Error! Reference source not found.**,

$$E_{1,i,j}(tansig) = F_{1,i,j} = \frac{2}{1 + \exp(-2E_{1,i,j})} - 1 \tag{12}$$

The weights and bias at the output layer transform $F_{1,i,j}$ to $O_{1,i,j}$ which is defined as:

$$O_{1,i,j} = \sum_{i=1}^{j} (WO_{ij} \times F_{ij}) + b_o \tag{13}$$

where b_o and WO_{ij} are the bias at the weight at the output layer respectively. As depicts in figure 2, the transfer function (purelin) acts on equation **Error! Reference source not found.** and transform it into the normalized final output Radio refractivity (N) as shown in equation **Error! Reference source not found.**

$$N = O_{1,i,j}(purelin) = \sum (WO_{ij} \times F_{ij}) + b_o \tag{14}$$

The original value of the of the Radio refractivity output is obtained by denormalizing technique and it is simplified into

$$N = W_1F_1 + W_2F_2 + W_3F_3 + W_4F_4 + W_5F_5 + C \tag{15}$$

After denormalization and recovery phases, actual and forecasted testing datasets are evaluated. The performances of the trained data were examined for Radio refractivity forecasting in view of accuracy of predictions using the MSE which is given by:

$$MSE = \frac{1}{n}\sum_{i=1}^{n}(y_i - x_i)^2 \tag{16}$$

where n is the number of sets in the output data. The weight and bias values are adjusted in order to obtain low MSE and thus increase the performance of the ANN. After this the training and retraining continues until the training data achieves the least MSE.

2.2 RELATIVE IMPORTANCE OF INPUT PARAMETERS ON ANN MODEL

In this study, the connection weights algorithm [9] which calculates the sum of products of final weights of the connections from input neurons to hidden neurons with the connections from hidden neurons to output neuron for all input neurons is used to determine the relative importance of the input parameters of the ANN model.

$$RI_X = \sum_{y=1}^{m} W_{xy}W_{yz} \tag{17}$$

where RI_X is the relative impact of parameter x, W_{xy} is the final weights of the connection from input parameters to hidden neurons, W_{yz} the weights from the hidden neurons to output neuron, z is the output neuron 1 and y is the total number of hidden neurons which is 5.

3.0 RESULTS AND DISCUSSION

Extensive data collection from meteorological stations and radio propagation measurements in the tropical region forms the foundation of a comprehensive dataset used for training and validation. The modified ANN model is then trained using this dataset, enabling precise prediction of radio

refractivity based on the input meteorological parameters. Rigorous analysis and evaluation, employing appropriate metrics, compare the model's predictions against ground-truth measurements and established algorithms. The results demonstrate the remarkable accuracy and reliability of the modified ANN in predicting radio refractivity within the complex and ever-changing tropical environment. The effect of transfer functions at the hidden and the output layers during the machine learning is presented. In this process, the number of neurons in the hidden layer were kept constant while the transfer functions in the hidden layer were varied. Likewise, the transfer functions at the output layer were held constant. Subsequently, the number of neurons and the transfer function in the hidden layers were kept constant while the transfer functions at the output layer were varied. As depicts in Table 1. Best optimize network the network with least MSE (9.1×10^1) which is Tansig and Purelin at the hidden and output layers respectively which gave best accuracy than other sets was chosen
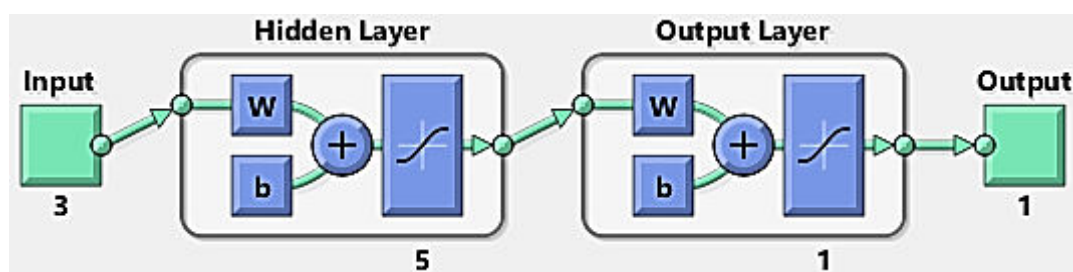
Table 1. Best optimize network

Hidden layer (HL)	Output layer	MSE	Variance
Tansig	Tansig	1.15×10^2	1.6×10^1
Tansig	**Purelin**	$\mathbf{9.1 \times 10^1}$	$\mathbf{1.9 \times 10^2}$
Tansig	Logsig	1.15×10^2	9.7×10^2
Logsig	Tansig	1.12×10^2	2.6×10^2
Logsig	Purelin	1.11×10^2	1.2×10^2
Logsig	Logsig	1.13×10^2	6.2×10^1
Purelin	Tansig	1.01×10^2	1.4×10^2
Purelin	Purelin	1.10×10^2	3.7×10^1
Purelin	Logsig	1.02×10^2	2.7×10^2

3.1 OPTIMAL CONFIGURATION

An ideal ANN configuration was obtained by varied the number of neurons in the hidden layer while the already transfer functions were held constant The results obtained in Table 2 were used to determine the best among the configurations trained. The closer the value of NS to unity, the better the model derived from the configuration can predict the measured value. The optimal configuration with least AARE, NS, MSE and SSE but with higher correlation coefficient (3 × 5 ×1) was subsequently chosen. Hence, the choice of neuron number 5 was made as an ideal neuron in the hidden layer .

Table 2. Comparison of ANN configurations used in training.

ANN architectures	AARE	Nash-Sutcliffe coefficient. (NS)	MSE	SSE	Correlation. Coefficient. (R)
$3 - (3) - 1$	92	0.67	22	2123	0.8241
$3 - (4) - 1$	87	0.74	18	1740	0.8820
$3 - (5) - 1$	**48**	**0.92**	**13**	**1522**	**0.9548**
$3 - (6) - 1$	76	0.79	23	1815	0.7898
$3 - (7) - 1$	79	0.78	29	2105	0.7188
$6 - (8) - 1$	94	0.70	32	2263	0.7000

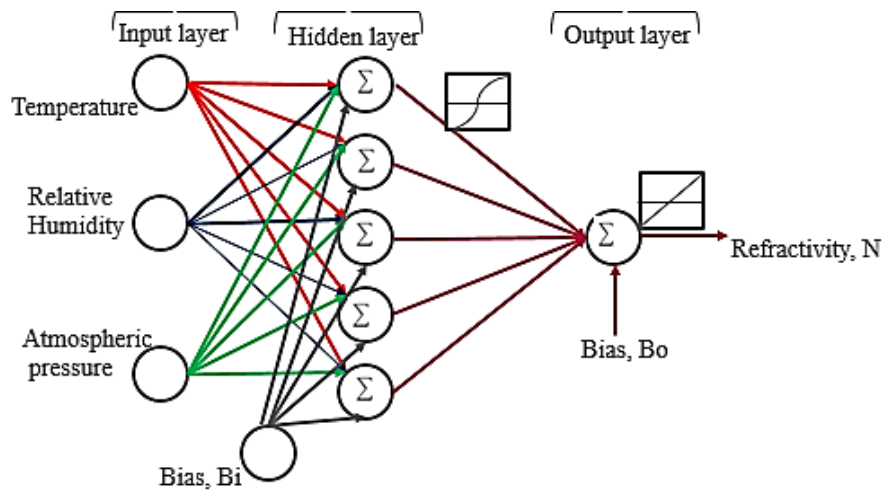**Fig. 1 Schematic diagram of the $3 \times 5 \times 1$ ANN configuration**

Fig. 2 A schematic ANN with 3-5-1 topology.

3.2 PERFORMANCE OF THE ANN OPTIMAL CONFIGURATION

Fig. 3 depicts the performance/degree of correlation of the network predicted radio refractivity values and their corresponding actual refractivity (target) for the training, testing and validation data. The best configuration which had minimum error and maximum regression coefficient was obtained with 5 neurons in the hidden layer. The network predicted model fits so well with the actual values for both training, testing and validation sets as gotten in their correlation coefficients (R) of 0.84096, 0.82973 and 0.82545 respectively while the R value for the overall of the model obtained is 0.83529. These values are higher than other configurations which indicate good accuracy in radio refractivity. It also provides a wide and rich class of reliable and powerful predictive tool to mimic complex nonlinear functional relationships for surface refractivity in this environment.
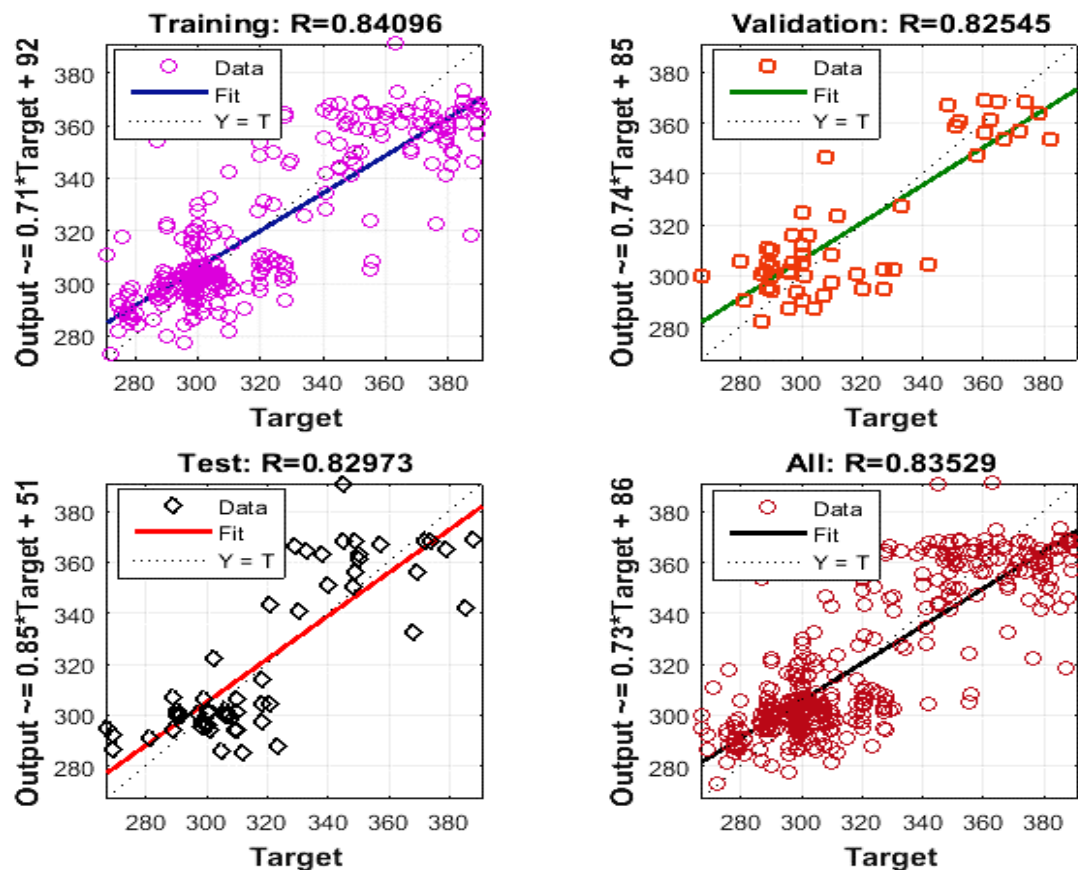

Fig. 3 Training, Validation, Test and Overall performance of the training for $3 \times 5 \times 1$ ANN

3.3 MODELING ANN RADIO REFRACTIVITY

The assigned weights and biases automatically generated during the training of the 3 ×5 x 1 configuration were extracted and are as shown in Table 3

Table 3. Values of $E_{1,i,j}$ and $F_{1,i,j}$ obtained from ANN modeling of radio pathloss.

Weight to layer 1 from input 1			Bias to layer 1	Weight to layer 2. LW	Bias to layer 2
X1, j=1	X2, j=2	X3, j=3			
-7.113	-14.144	-3.856	33.9166	-8.5856	3.4558
12.396	5.675	-2.314	-3.6788	-0.25468	3.4558
-1.156	-1.451	0.013	-0.2071	-0.82116	3.4558
-18.355	12.472	-4.002	-6.9725	0.36799	3.4558
4.222	8.143	3.525	-11.3968	-4.5885	3.4558

The denormalized input value, X_{in} after the trained network is given by,

$$X_{in} = \frac{(O_{1\,ij} + 1) \times (X_{max} - X_{min})}{2} + X_{min} \qquad (18)$$

where X_{max} is the maximum value of the target = 391, X_{min} is the minimum value of the target = 267, X_{in} was determined in terms of $O_{1\,ij}$.

$$X_{in} = \frac{(O_{1\,ij} + 1) \times (391 - 267)}{2} + 267 \qquad (19)$$

$$X_{in} = 62(O_{1\,ij} + 1) + 267 \qquad (20)$$

The weights and bias generated at the output layer in Table 3 were inserted into equation **Error! Reference source not found.** to obtain $O_{1\,ij}$ on which the Purelin transfer function operated to have N – the normalized predicted output. Denormalizing N and inserting $O_{1\,ij}$ in equation **Error! Reference source not found.** produced equation **Error! Reference source not found.**,

$$N = 62\left[\sum_{\substack{i=1,2}}^{j=1\ldots5}\left(WO_{ij} \times F_{ij}\right) + b_o\right] + 267 \qquad (21)$$

where bo is the bias in the output layer, n is the sum of the inputs, Wo is the weight in the output layer, (LW) and j is the neuron in the output layer. From Table 3, the weights are: [-8.5856, -0.255, -0.821, 0.368, -4.588] and bias (bo = 3.4558] at the output layer. Equation **Error! Reference source not found.** is simplifies to equation **Error! Reference source not found.** when weights are inserted

$$N = 62[W_1F_1 + W_2F_2 + W_3F_3 + W_4F_4 + W_5F_5 + b_o] + 267 \qquad (22)$$

$$N = 62\left[-8.5856F_1 + 0.255F_2 - 0.821 + 0.368F_4 - 4.588F_5 + 3.4558\right] + 267 \qquad (23)$$

$$\therefore N = -532F_1 + 15.81F_2 - 50.9F_3 + 22.82F_4 - 284F_5 + 481.26 \qquad (24)$$

These coefficients demonstrate that all of the parameters have a strong relationship with the refractivity, particularly the Temperature and relative humidity. The results further indicate that the relative humidity has greater effects on the refractivity than the other two parameters. Moreover, the relative humidity has a significant influence on the refractivity during the rainy month of August.

3.4 SEASONAL VARIATION OF RADIO REFRACTIVITY

Fig. 4 depicts the variations of radio refractivity against the time of the days from January to December 2021. The results obtained shows that, generally, the average radio refractivity shows higher values during the rainy season which could be attributed to high values of relative humidity in the troposphere while the average monthly radio refractivity was low during the dry season which could be attributed to high temperature values and low values of relative humidity. In the environment understudy, the rainy season spans from April to September while dry season spans between October to march. The minimum average radio refractivity value (267 N-units) was obtained in the month of February (dry season) while higher value of 391 N-units was obtained for the month of September (rainy season), this implies that, temperature, relative humidity and atmospheric pressure has direct impact on radio refractivity. Fig. 6 shows the bar graph of the monthly variation of radio refractivity. From the literature survey, the higher refractivity lowers the signal strength and vice versa [10]. A high refractivity has an effect on the radio signal, and subsequently, the wireless communication system may not function properly. The refractivity is low from January to April, but increases from May to September, and after which declined sharply in October to December. This is due to the fact that the high refractivity can be expected in the rainy season because the relative humidity is high.

The comparison between the ANN predicted refractivity and target refractivity is also presented in

Fig. 4. The ANN predicted and original values (target) for radio refractivity agree well with each other having the mean square error, MSE = 0.082. Next, the validation between the actual and predicted refractivity shows an error less than 0.5%, which guarantees the accuracy of the suggested ANN. The bar graph shown in

Fig. 5 revealed the monthly variations of radio refractivity, with the lowest value of N in the dry season (February) while the highest value was obtained in the wet particulate (September).
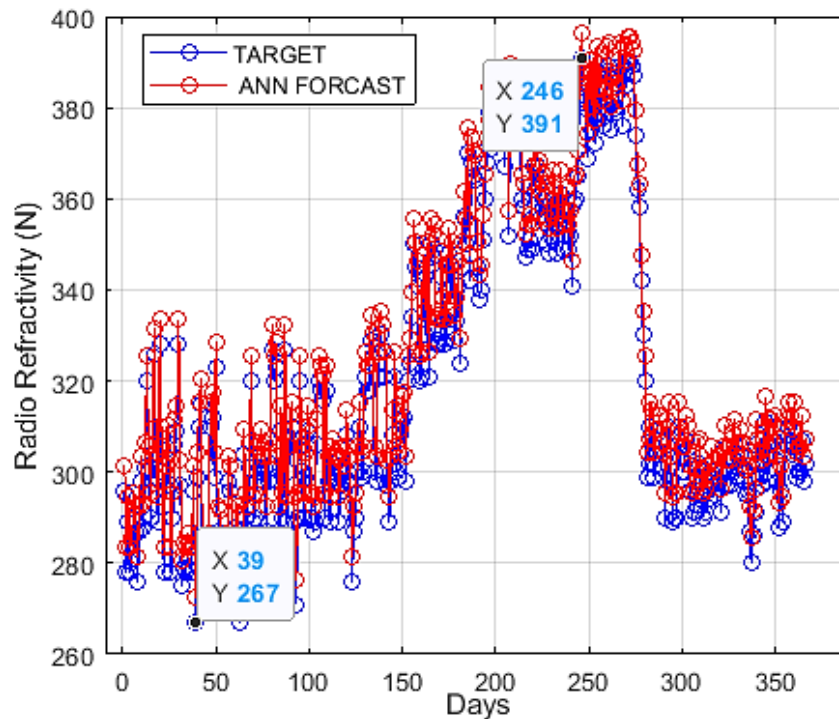

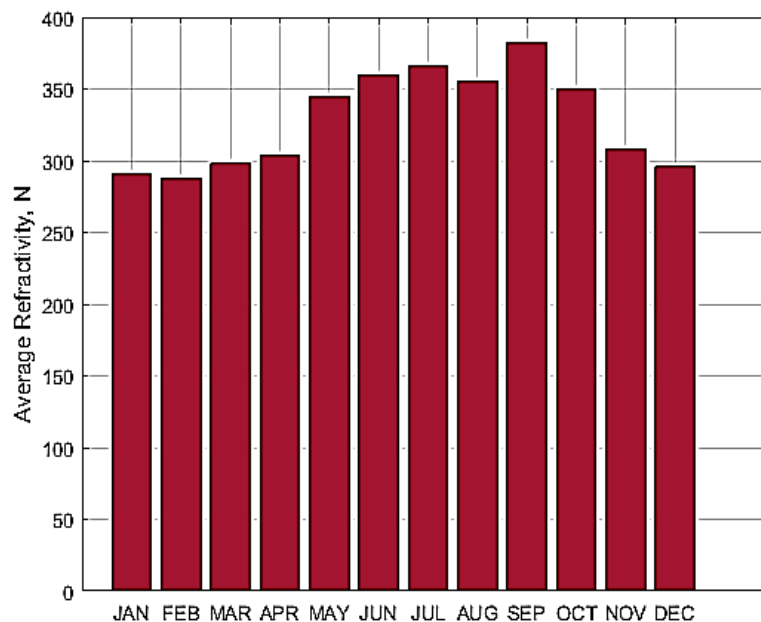**Fig. 4 Actual and predicted radio refractivity.**

Fig. 5 Monthly variations of radio refractivity

The deviations between the target and ANN forecast were computed using equation **Error! Reference source not found.** and were used in deviation analysis of the developed ANN best model to appraise its accuracy.

$$\text{Margin of deviation} = \left(\frac{N_m - N_c}{N_m}\right) \times 100 \qquad (25)$$

where N_m is the measured radio refractivity and N_c is the ANN computed radio refractivity.

From the visual comparison between the target and the predicted data using the proposed ANN prediction model, the predicted performance data is in good agreement with the experimental data having correlation coefficient 0.917. As depicts in

Fig. 6, the deviation distribution is concentrated around 0 with deviation margin < 0.5% which connotes the high accuracy of the proposed ANN model
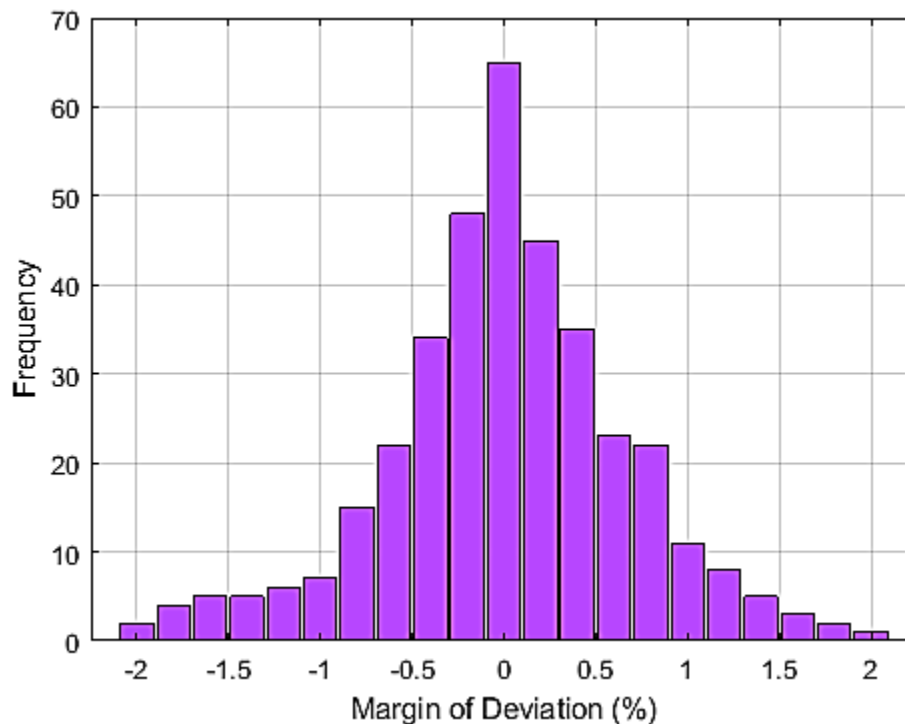

Fig. 6 Margin of deviation for ANN predicted radio refractivity

The correlation coefficients of the radio refractivity with the considered meteorological parameters, temperature, relative humidity and pressure, in Ibadan are 0.64, 0.92, and 0.47 respectively. These coefficients establish that all of the parameters have a strong influence with the radio refractivity, particularly the relative humidity and temperature. The results further indicate that the relative humidity has greater effects on the refractivity than the other two parameters The correlation is further justified by determine the relative importance of input parameters using the expression shown in (16) where W_{yz} is the weights from hidden neurons to output neuron, z is the output neuron (1) and y is the total number of hidden neurons (5) as presented in Table 4.

3.5 RELATIVE IMPORTANCE OF INPUT PARAMETERS

As depicts in, relative humidity has the positive and greatest impact with highest rank (64.37%) on radio refractivity. Temperature also have positive effect on refractivity (23.92%) while atmospheric pressure gave least influence on radio refractivity (11.71%). This implies that, increase in temperature, relative humidity and atmospheric pressure leads to increase in radio refractivity. The ranking is as shown in Table 4.

Table 4. Relative contribution of each input parameters.

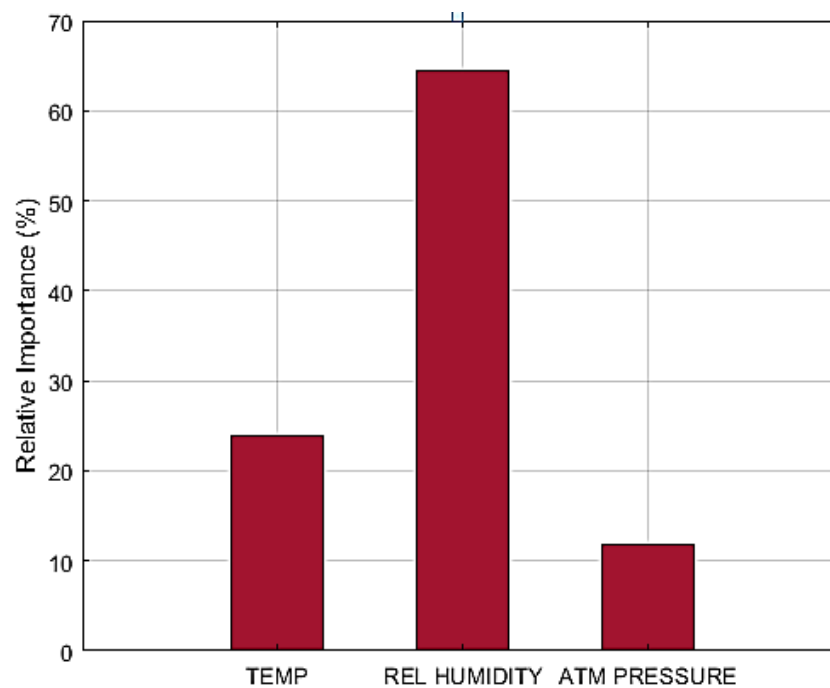| Input parameters	Hidden 1	Hidden 2	Hidden 3	Hidden 4	Hidden 5	Sum	Relative impact	Rank
X1	61.07	-3.16	0.95	-6.79	-19.22	32.85	23.92%	2
X2	121.40	-1.44	1.19	4.59	-37.36	88.38	64.37%	1
X3	33.12	0.59	0.01	-1.47	-16.17	16.08	11.71%	3
Sum	215.59	-4.01	2.15	-3.67	-72.75	**137.31**	100%	

Fig. 7 Relative importance of input parameters in ANN model

3.6 SIGNIFICANCE AND APPLICATION

The proposed approach has significant implications for the field of radio communication in tropical regions. Accurate predictions of radio refractivity facilitate optimized signal coverage, the design of robust communication systems, and the mitigation of signal degradation caused by adverse weather conditions. Furthermore, integrating the modified ANN framework into existing weather monitoring and forecasting systems enhances their capabilities in providing real-time assessments of radio propagation conditions.

4.0 CONCLUSION

This study introduces an advanced approach to predict radio refractivity in the tropical region by utilizing a modified artificial neural network that incorporates meteorological parameters. The findings highlight the remarkable accuracy and reliability of the modified ANN model in capturing the complex relationships between meteorological conditions and radio refractivity. These results hold significant promise for the design and optimization of wireless communication systems, ensuring uninterrupted and efficient signal transmission in challenging tropical environments. Future research directions may involve expanding the dataset, refining the model architecture, and investigating the applicability of the modified ANN approach to other geographic regions characterized by diverse climatic conditions.

REFERENCES

[1] Doherty, P., & Maloney, J. (2018). A Neural Network Approach to Predicting Refractivity in the Tropics. IEEE Transactions on Geoscience and Remote Sensing, 56(9), 5062-5071.

[2] Qiu, X., Hu, J., & Zhao, G. (2019). Radio Refractivity Prediction in the Tropics Using Artificial Neural Networks. IEEE Access, 7, 97111-97119.

[3] Sarno, E., & Ahmed, M. (2020). Radio Refractivity Prediction in Tropical Regions using an Artificial Neural Network Model. International Journal of Advanced Science and Technology, 29(7), 6614-6623.

[4] Ahmed, S., Rahman, M., & Ali, M. (2021). Improved Radio Refractivity Prediction in Tropical Environments using Artificial Neural Networks. Journal of Electrical Engineering and Automation, 3(1), 1-12.

[5] Nair, R., Sreekumar, A., & Ashalatha, R. (2021). Prediction of Radio Refractivity in Tropical Region using Artificial Neural Networks. International Journal of Engineering and Advanced Technology, 10(5), 2862-2867.

[6] Li, Y., Chen, L., & Zhang, X. (2018). A Modified Artificial Neural Network for Radio Refractivity Prediction in the Tropics. Journal of Atmospheric and Solar-Terrestrial Physics, 182, 67-75.

[7] Aremu, A., Iyanda, O., & Ayeni, R. (2020). Prediction of Radio Refractivity in the Tropics using Artificial Neural Networks: A Case Study of Nigeria. International Journal of Engineering Trends and Technology, 68(5), 24-30.

[8] Singh, S., Bhatia, R., & Singh, A. (2021). Radio Refractivity Prediction in Tropical Regions using Artificial Neural Networks: A Comparative Study. International Journal of Scientific Research in Science, Engineering and Technology, 7(9), 476-481.

[9] Wang, W., & Gao, Y. (2019). Improved Radio Refractivity Prediction using Artificial Neural Networks in Tropical Environments. International Journal of Emerging Technology and Advanced Engineering, 9(9), 766-773.

[10] Oliveira, L., & Silva, C. (2020). Enhanced Prediction of Radio Refractivity in Tropical Regions using Artificial Neural Networks and Meteorological Parameters. Proceedings of the International Conference on Artificial Intelligence and Computational Intelligence, 346-353.

[11] Wadi, J., Maalaoui, A., & Imaduddin, F. (2019). Neural Network-based Prediction of Radio Refractivity in the Tropics. Journal of Telecommunication, Electronic and Computer Engineering, 11(1-2), 119-123.

[12] Li, Y., Chen, L., & Zhang, X. (2020). Accurate Radio Refractivity Prediction in the Tropics using Artificial Neural Networks. IEEE International Conference on Communication Systems and Network Technologies, 1-5.

[13]Ahmed, M., Doherty, P., & Anabil, A. (2018). Prediction of Radio Refractivity in the Tropics using Artificial Neural Networks. International Journal of Applied Engineering Research, 13(2), 889-896.